Trapped hole Fe^{3+} centres in layered $CdCl_2$:Fe crystals

1994 J. Phys.: Condens. Matter 6 2619

(http://iopscience.iop.org/0953-8984/6/13/019)

J. Phys.: Condens. Matter 6 (1994) 2619–2630. Printed in the UK

Trapped hole Fe^{3+} centres in layered $CdCl_2$:Fe crystals

S V Nistor†, E Goovaerts and D Schoemaker
Physics Department, University of Antwerp (UIA), B-2610 Antwerpen–Wilrijk, Belgium

Received 4 January 1994

Abstract. EPR spectra attributed to Fe^{3+} centres, produced by hole trapping at substitutional Fe^{2+} ions, are observed below 250 K, in x-ray-irradiated $CdCl_2$ single crystals doped with 0.1 mol% Fe. The zero-field-splitting parameter b_2^0 decreases from 0.0818 cm^{-1} at 13 K to 0.0736 cm^{-1} at 225 K. Its absolute value and temperature dependence are well described by the superposition model of Newman, assuming a temperature-dependent Coulomb contraction of the Cl^- ligands sandwiching the Fe^{3+} ion.

1. Introduction

Many metal dihalide (MX_2) compounds exhibit a layered structure, consisting of metal (M^{2+}) cation layers sandwiched between layers of halogen (X^-) anions [1]. The interest in such structures is due to the strong anisotropy of their physical properties resulting from the different nature of the chemical bonding, which is ionic and covalent inside the sandwich and of the Van der Waals type between the anion layers from successive sandwiches. One of the consequences is that the crystals cleave easily in thin sheets, parallel to the ion planes.

$CdCl_2$ is a typical layered compound of the type $\ldots Cl^-Cd^{2+}Cl^-\ldots$. Its crystal structure [2, 3] is rhombohedral and belongs to the space group $R\bar{3}m$ (D_{3d}^5) with cell parameters $a = 0.38459$ nm and $c = 1.74931$ nm at room temperature (RT). The Cd^{2+} cations are located in the octahedral interstices of the Cl^- layers (figure 1). The d/a ratio, where d is the thickness of the sandwich, differs in general from the $d/a = 0.816$ value, which corresponds to the cubic arrangement of the six nearest Cl^- ions. For $CdCl_2$ the Cd^{2+}–Cl^- distance is 0.2637 nm, the Cl^-–Cl^- distance is 0.38459 nm between ions of the same plane and 0.3609 nm between nearest Cl^- ions in neighbouring planes [3]. The resulting separation ($d = 0.2916$ nm) corresponds to a compression along the trigonal c-axis. Moreover the d/a ratio is temperature dependent, as shown from EPR studies on substitutional Mn^{2+} ions [4].

The relative ease with which large, pure or doped $CdCl_2$ single crystals can be grown, as well as their good dielectric and transparency properties, has determined their frequent use as host lattices in various studies such as EPR spectroscopy of Mn^{2+} [4, 5], V^{2+} [6, 7], Co^{2+} [8, 9], Fe^+ [10], Ni^{2+} [10, 11] or Cu^{2+} [10, 12, 13, 14] transition ions, low-dimensional magnetism [15], luminescence and related properties [16, 17], or dielectric properties [18]. However, very few data concerning the intrinsic or radiation-induced defects in pure or doped $CdCl_2$ crystals have been published as yet [19].

The present paper reports the results of an EPR study of Fe^{3+} centres produced by x-ray irradiation of $CdCl_2$:Fe crystals. Our results show that the Fe^{3+} centres are produced by hole

† On leave from the Institute of Atomic Physics (IFTM), Bucuresti, Romania.

0953-8984/94/132619+12$19.50

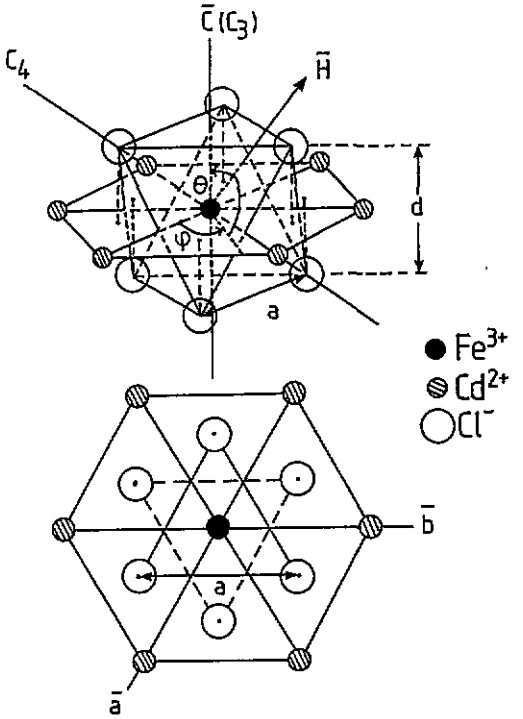

Figure 1. The crystalline surroundings of the substitutional Fe^{3+} ion in $CdCl_2$. The perspective drawing for $d/a = 0.816$ (top), and a view along the trigonal axis (bottom) are presented. The orientation of the magnetic field, as considered in the text, is also presented.

trapping at substitutional Fe^{2+} ions, without directly involving in their stabilization lattice defects, such as vacancies or interstitials. The presence of a strongly temperature-dependent second-order zero-field-splitting (ZFS) term b_2^0 is reported. Its value, about two orders of magnitude larger than that previously reported for the isoelectronic Mn^{2+} impurity ions, is explained by the Coulomb attraction of the nearest Cl^- ligands to the extra positive charge of the Fe^{3+} ion. This effect seems to be favoured by the weak binding of the surrounding Cl^- ligands to the next layer of Cl^- ions, characteristic of a layered structure.

2. Experimental details

Pure and Fe-doped (0.1 mol%) single crystals of $CdCl_2$ have been grown in a Cl_2 atmosphere by the Bridgman technique in sealed fused silica ampoules. As starting material use was made of Extrapure grade (Merck) $CdCl_2 \cdot H_2O$, which was initially dehydrated in an oven at 180 °C. The resulting material was finely ground, loaded in the ampoules and thoroughly dried under vacuum (10^{-2} mm Hg) at 250 °C, until a sharp drop in pressure was observed. The removal of the remaining O- and OH^--related molecules from the crystal was achieved by flushing the content of the ampoules with a stream of Ar gas containing CCl_4 and slowly increasing the temperature up to 800 °C. The chlorinating agent was introduced into the substance by means of a thin fused silica tube. After the reaction was over, i.e., the melt surface became convex, the thin tube was withdrawn and the ampoule was sealed off and cooled. The Fe-doped samples were obtained by adding in the melt, before sealing the

ampoule, H-reduced Fe powder. The ampoule was sealed off after the whole amount of Fe had reacted with the Cl_2, which could be checked visually. By this doping procedure the contamination of the crystal with O, or iron oxide, is practically eliminated. The crystal growth was performed in a two-zone furnace, with a lowering speed of 2 mm h^{-1}. The resulting crystals were homogeneous and transparent, easily cleaving in sheets with their faces perpendicular to the *c*-axis.

Samples for EPR measurements, of about 3× 3× 8 mm^3 size, were cut with a sharp razor blade from cleaved, 3 mm thick, crystal sheets. Due to the weak mechanical properties of the $CdCl_2$ crystals the resulting samples exhibited the tendency to bend and to chip at the edges, reducing the accuracy of the EPR measurements.

The EPR investigations were performed with an X-band spectrometer, model ESP-300E from Bruker, equiped with a gas-flow cryogenic cooling system allowing operation in the 10–300 K temperature range. The x-ray irradiations were performed from 80 K upward, using a Siemens tube with W anode, operating at 50 kV and 50 mA. Optical absorption measurements were performed with a Cary-5 spectrophotometer equiped with optical cryostats. Other experimental details concerning *in situ* thermal and optical treatments are the same as in [20].

3. Results

3.1. Electron paramagnetic resonance experiments

The as-grown samples of Fe-doped $CdCl_2$ exhibited EPR transitions attributed to substitutional Mn^{2+} and Co^{2+} ions [4, 5, 8] ions. The Mn^{2+} transitions were visible in the whole temperature range under investigation, with a strong saturation at 10 K, for microwave powers of 1 mW. The EPR transitions from the Co^{2+} ions could be observed only at temperatures below 30 K. No saturation was observed at $T = 10$ K for microwave powers of 100 mW. The EPR transitions of both Mn^{2+} and Co^{2+} ions were also visible with comparable intensity in the undoped $CdCl_2$ samples. Thus they originate from the raw $CdCl_2{\cdot}H_2O$ material employed for our study. The EPR spectra of both Mn^{2+} and Co^{2+} impurities were not affected in any discernible way by the x-ray irradiations performed at either 80 K or at RT.

New EPR lines attributed to Fe^{3+} centres, strongly anisotropic both in position and intensity, have been observed at $T < 250$ K after a relatively short (15 min) x-ray irradiation at liquid nitrogen temperature (LNT) or RT. The concentration of the Fe^{3+} centres obtained by x-ray irradiation at RT is about 10 times larger than to the concentration resulting from an x-ray irradiation, otherwise in the same conditions, at 80 K. Pulse annealing experiments performed on samples x-ray irradiated at 80 K did not show any sizable change in the concentration of the Fe^{3+} centres after subsequent annealings up to RT.

The EPR spectra of a $CdCl_2$:Fe sample x-ray irradiated at RT, for the magnetic field parallel and perpendicular to the *c*-axis, as well as the angular variation obtained by rotating the magnetic field in the plane containing the trigonal *c*-axis and the projection of a cubic axis in the *ab*-plane, are presented in figure 2. Although the most intense EPR lines are still visible at $T = 240$ K, the whole spectrum begins to broaden and lose intensity for temperatures above 170 K. No saturation effects were detected at $T = 10$ K for microwave powers of 20 mW. Under the same conditions the EPR lines of the isoelectronic Mn^{2+} ions were strongly saturated, which offered us the possibility of observing the $M = \frac{1}{2} \longleftrightarrow -\frac{1}{2}$ transition (for $H \parallel c$) of the Fe^{3+} centres, otherwise obscured by the more intense Mn^{2+} lines. The above experimental observations suggest that the Fe^{3+} ions exhibit a stronger

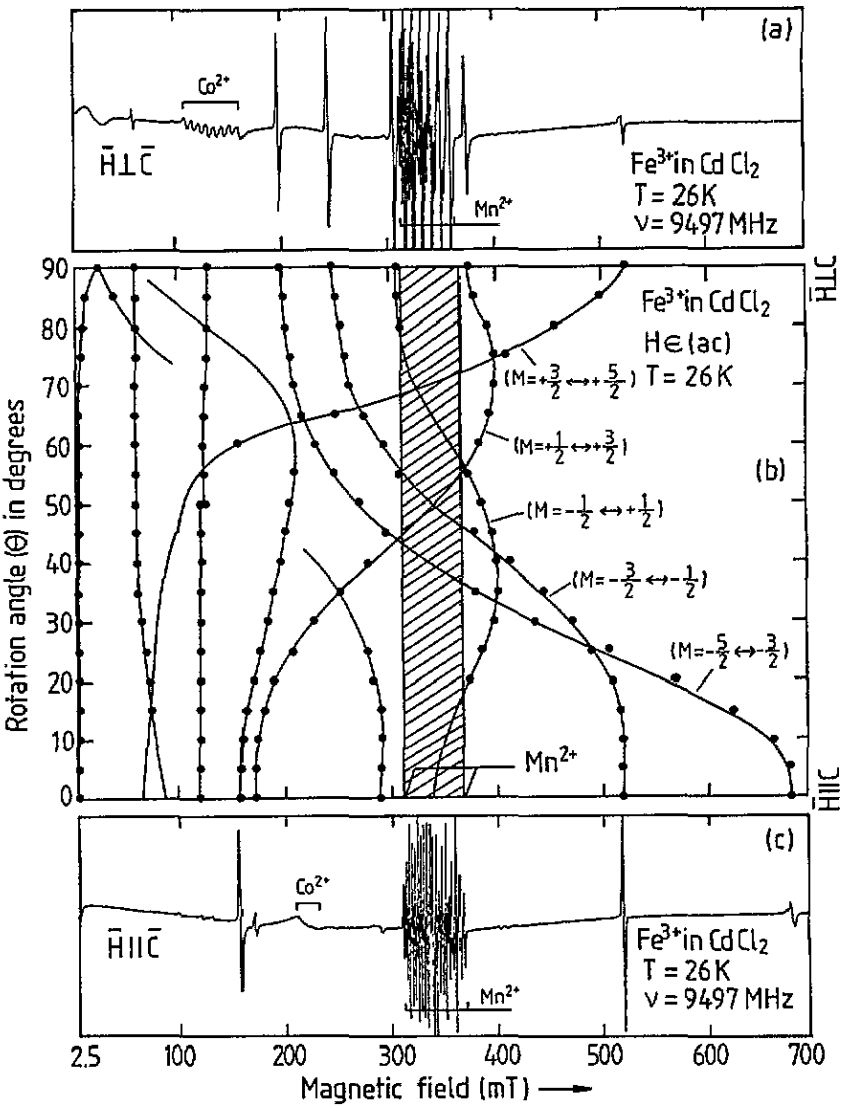

Figure 2. EPR spectra at $T = 26$ K of the Fe^{3+} centre in $CdCl_2$, for the magnetic field (a) perpendicular ($\phi = 0$) and (c) parallel to the trigonal c-axis. The experimental data, represented by dots, are compared in (b) to the calculated angular variation (continuous lines) of the various EPR transitions with normalized transition probabilities larger than 0.05, calculated with the spin Hamiltonian parameters of table 1. The various transitions are identified with their quantum numbers corresponding to the high-field approximation for $H \parallel c$.

spin–lattice coupling than the isoelectronic Mn^{2+} ions.

As shown in figure 2, the EPR spectrum attributed to the Fe^{3+} centres extends from zero to about 680 mT, with a half width of the various lines of 2.0±0.2 mT for the magnetic field parallel or perpendicular to the c-axis in the best samples. (The lowest-field line observed for $H \perp c$ is the only exception.)

Due to their hygroscopic character and to the high density of dislocations induced by cutting, we were not able to obtain by x-ray diffraction oriented samples, i.e., samples

with a known orientation of the long (rotation) axis relative to the a or b crystal axes. The resulting difficulty has been circumvented by cutting for the EPR measurements several samples from the same crystal sheet, with the long axis at different known angles with respect to an arbitrary direction x in the ab-plane. As a result, by rotating the sample around its long axis (kept perpendicular to the magnetic field), it has been possible to obtain angular dependences of the EPR spectra with the magnetic field rotated in various planes containing the c-axis and intersecting the ab-plane at known azimuthal angles (ϕ) from x.

The same general angular variation of the EPR lines attributed to the Fe^{3+} centres, associated with an axial symmetry around the c-axis (figure 2(b)), has been found for all samples. The relatively small variations in the line positions observed between the various samples at magnetic field orientations away from the main crystal axes have been accounted for by the contribution of the $B_4^3O_4^3$ trigonal term in the spin Hamiltonian. This aspect will be discussed latter. The axial symmetry of the Fe^{3+} centres has been further confirmed by the observed isotropic character of the EPR lines for the rotation of the magnetic field in the ab-plane. (The very small anisotropy, of less than 0.5 mT, is due to the same trigonal contribution.)

It has been found that for rotation angles of the magnetic field of more than 15° away from the main axes, in the angular range where the line positions are changing rapidly, the individual linewidths increase. Such a behaviour has also been reported in the EPR spectra of Ni^{2+} ions[11] and attributed to a spread of the local axes (mosaicity effect). Besides the broadening effect we have observed in the same angular range, in some of our samples, a splitting of the EPR lines attributed to the Fe^{3+} centres into several components. Their number, separation and relative intensities changed erratically from sample to sample. A careful examination of the samples employed in the EPR measurements has shown that, during the cutting from single-crystal sheets, a partial splitting of the sample in several pieces cannot always be avoided . Although the resulting pieces were still attached together, their separation was further enchanced by cooling down during the EPR measurements. Because the crystal pieces were quasi parallel, the resulting line-splitting effect was observed only for those orientations of the sample in the magnetic field where the EPR lines were changing rapidly. The above interpretation of the observed splitting is supported by the observation that the angular variation of the average line position was reproducible from sample to sample. Unfortunately these effects also resulted in a diminished accuracy of the spin Hamiltonian parameters.

The EPR spectrum attributed to the Fe^{3+} centres is fully described by the following spin Hamiltonian corresponding to trigonal symmetry:

$$\mathcal{H}_s = g\mu_\beta \boldsymbol{H}\cdot\boldsymbol{S} + B_2^0O_2^0 + B_4^0O_4^0 + B_4^3O_4^3 \qquad (1)$$

with the usual notations [21], where $S = \frac{5}{2}$. The electronic Zeeman term, which was found to be isotropic, as expected for an S-state ion, and the second-degree ZFS term B_2^0 are the main contributors. The other two ZFS terms B_4^0 and B_4^3 are much smaller, and therefore determined with less precision.

A rough estimate of the spin Hamiltonian parameters has been initially obtained from an analysis of the high-field lines for the $\boldsymbol{H} \parallel \boldsymbol{c}$ and $\boldsymbol{H} \perp \boldsymbol{c}$ orientations, using the energy level formulae[22] in the strong-magnetic-field approximation, to the second order of perturbation. The resulting values were further employed as initial parameters in a fitting procedure based on a full diagonalization of spin Hamiltonian (1).

The $B_2^0O_2^0$ and $B_4^0O_4^0$ terms have cylindrical symmetry around the c-axis. Their contribution can be accurately determined from the line positions for $\boldsymbol{H} \parallel \boldsymbol{c}$ and $\boldsymbol{H} \perp \boldsymbol{c}$, which are also less affected by the quality of the measured samples. At these orientations

the contribution from the trigonal $B_4^3O_4^3$ term was found to be negligible, as reflected in the unchanged line positions measured in different samples at the same temperature.

To distinguish the effect of the trigonal term, as well as to determine its magnitude, measurements in other directions are required. The effect of the $B_4^3O_4^3$ term is most clearly seen as a small variation ($\approx$ 10 mT), as a function of the azimuthal angle ϕ, in the line positions of the $M = \frac{1}{2} \longleftrightarrow -\frac{1}{2}$ and $M = \frac{1}{2} \longleftrightarrow \frac{3}{2}$ transitions at $\theta = 35°$ and $\theta = 70°$, respectively, where θ is the angle between the magnetic field and the trigonal c-axis. The analysis requires in principle the knowledge of the cubic ξ, η, ζ axes, or, equivalently, the orientation of the magnetic field projection in the ab-plane (the ϕ angle) for at least one set of experimental data. As previously mentioned, we have circumvented this condition, which requires the knowledge of the a- (or b-) axis, by using in our fitting procedure several sets of data taken with the magnetic field at the same angle θ from the c-axis but at various known angles ϕ_i from an arbitrary direction x in the ab-plane. As such it has been possible to obtain not only the value of the B_4^3 parameter but also the absolute angle ϕ for each set of data, i.e., the orientation relative to the projection of the cubic axis ξ in the ab-plane .

Table 1. Spin Hamiltonian parameters of the Fe^{3+} centre in $CdCl_2$ at two temperatures. The ZFS parameters are given in 10^{-4} cm^{-1}, with accuracies of ± 0.2 for b_2^0, ± 0.9 for b_4^0 and ± 30 for b_4^3. The g-value has been determined with an accuracy of ± 0.001. The corresponding parameters for the Mn^{2+} in $CdCl_2$ and for the Mn^{2+} and Fe^{3+} in $CaCl_3$ are given for comparison.

System	T (K)	g	b_2^0	b_4^0	b_4^3
Fe^{3+} in $CdCl_2$ [a]	26	2.008	815.7	−13.9	−400
Fe^{3+} in $CdCl_2$ [a]	225	2.008	736.0	−10.6	−302
Mn^{2+} in $CdCl_2$ [b]	20	2.0015	14.8	> 0.5	—
Mn^{2+} in $CaCO_3$ [c]	77	2.002	77.6	2.63	|1140|
Fe^{3+} in $CaCO_3$ [d]	77	2.003	963.0	−38.78	|875|

(a) This work.
(b) [5].
(c) [31].
(d) [32].

The spin Hamiltonian parameters that gave the best fit to all experimental data are presented in table 1, in terms of the more usual parameters:

$$b_2^0 = D = 3B_2^0 \qquad b_4^0 = \frac{F-a}{3} = 60B_4^0 \qquad b_4^3 = \frac{-20\sqrt{2}}{3}a = 60B_4^3. \tag{2}$$

As shown in figure 2(b) for one particular plane ($\phi = 0$), the calculated angular dependence of the line positions for the various allowed transitions is in good agreement with the experimental data. Although not explicitly shown, the calculated transition probabilities have been found to agree with the intensities of the observed EPR lines within ±15%. Moreover, the strong intensity variation of the low-field lines ($H < 200$ mT) with the angle ϕ, calculated with the spin Hamiltonian parameters of table 1, has been found to be in agreement with the identification of the cubic axes derived from the line positions, previously described.

The EPR spectra of the Fe^{3+} centres recorded at various temperatures exhibit strong changes in their line positions. A quantitative analysis by the above-described procedure resulted in the temperature dependence of the b_2^0 and b_4^0 parameters presented in figures 3 and 4, respectively. Both b_2^0 and b_4^0 parameters exhibit a linear temperature dependence for $T > 60$ K. The g-parameter has been found to be isotropic and temperature independent

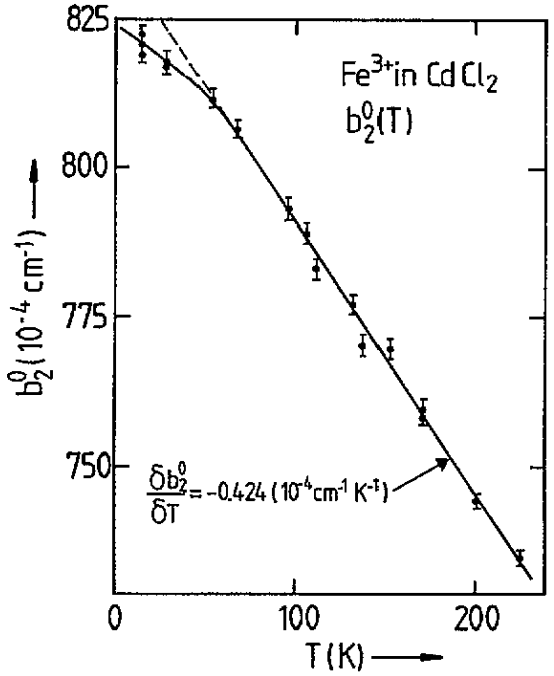

Figure 3. The temperature dependence of the second-order ZFS parameter b_2^0 for the Fe^{3+} centre in $CdCl_2$. Both experimental data and the best-square-fit curve are shown.

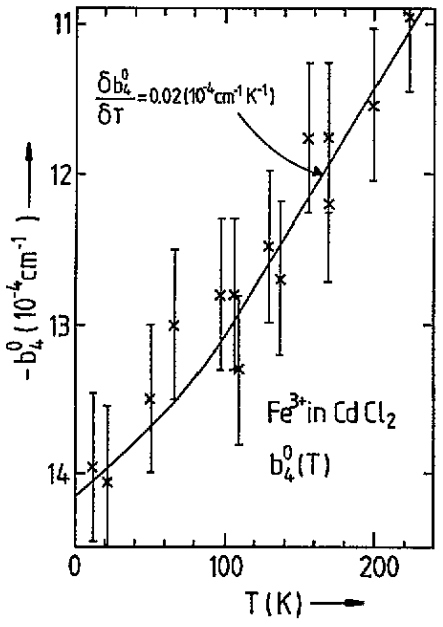

Figure 4. The temperature dependence of the fourth-order ZFS parameter b_4^0 for the Fe^{3+} centre in $CdCl_2$. Both experimental data and the best-square-fit curve are given.

in the limits of experimental errors. The temperature variation of b_4^3 was found to be

comparable to the experimental errors involved in the determination of its absolute value. Consequently any temperature dependence presentation would have been doubtful. It is, however, worthwhile mentioning that the relation $b_4^3 \simeq 20\sqrt{2}b_4^0$ seems to hold in the whole measured temperature range.

It has been impossible to determine with certitude, in the temperature range available, the sign of b_2^0 by measuring the relative intensities of the various fine-structure components of the EPR spectrum. However, by comparison with the corresponding value of the isoelectronic Mn^{2+} ion [5] it is concluded that $b_2^0 > 0$. This assumption is further supported by the analysis of the b_2^0 parameter with the superposition model (SM).

3.2. Optical absorption measurements

Optical absorption measurements performed at 80 K, in the 210–1500 nm range, on $CdCl_2$:Fe samples of various thicknesses, did not reveal any new absorption bands that could be associated with the Fe^{3+} centres produced by x-ray irradiation at RT or 80 K. This is not entirely surprising, because it is known that for the $3d^5$ configuration ions the optical absorption bands are weak.

4. Discussion

The analysis of the new EPR spectrum observed in x-ray-irradiated $CdCl_2$:Fe crystals demonstrates that the resulting paramagnetic centres consist of $Fe^{3+}(3d^5)$ ions in the ^6S ground state, subjected to an axial (trigonal) crystal field parallel to the c-axis.

The appearance of Fe^{3+} ions after x-ray irradiation raises the question of what valence and localization the Fe takes in the as-grown crystal, as well as how the Fe^{3+} centre is formed.

In a site with octahedral symmetry the ground state $^4F_{3/2}$ of the $3d^7(Fe^+)$ configuration is split into a Γ_2 singlet and two triplets Γ_4 and Γ_5, the Γ_4 triplet being the lowest [21]. The spin–orbit coupling lifts the 12-fold degeneracy of the Γ_4 state leaving a Kramers doublet as the ground state. The g-value of this ground state with fictitious spin $S = \frac{1}{2}$ is $g \simeq 4.33$. The effect of lower-symmetry crystal fields consists [21, 23] in mixing excited states into the ground state, the sum of the g_i-components being $\simeq 13$. Such Fe^+ spectra have been observed at $T < 35$ K in alkali chlorides such as NaCl[24, 25] and LiCl[26], either as isotropic lines with $g \simeq 4.3$ (unperturbed cubic sites), or anisotropic lines with $g_i > 2$ (vacancy-perturbed sites with tetragonal or orthorhombic symmetry). No such spectra have been observed in our as-grown $CdCl_2$:Fe samples.

In an octahedral crystal field the ^5D ground level of the $Fe^{2+}(3d^6)$ ion is split into a Γ_5 triplet and a Γ_3 doublet. The spin–orbit coupling further splits the lowest-lying Γ_5 level into a triplet, quintet and septet, the triplet being the lowest. Its effective g-value is shown [21] to be $g > 3$. If Fe^{2+} were substitutional at a site with D_{3d} symmetry, as in $CdCl_2$, the triplet would split further into a singlet and a doublet. The position of the lowest level and the resulting g-values would depend on the sign and magnitude of the trigonal component. The g-value of Fe^{2+} in NaF was found [27] to be $g = 3.42$. An asymmetrical EPR line, at $g_{\|} = 7.4$, attributed to the Fe^{2+} ions has been observed [10] in $CdCl_2$. We found no evidence of such an EPR spectrum in our as-grown or x-ray-irradiated samples. This is not altogether surprising considering the past experience in observing EPR spectra from non-Kramers Fe group ions. The presence of orbital moment in the ground state results in strong spin–lattice coupling and strain-induced broadening effects, which can make the EPR line unobservable. It is also possible that the crystals employed in [10] contained Fe_2O_3

particles resulting from the reaction at high temperature of the iron chloride with traces of O_2 and H_2O, during the crystal growth in vacuum or in an inert atmosphere. Such particles can give broad, asymmetrical EPR lines at $g > 4$, as seen [28] in Fe-doped alkali halide crystals grown in vacuum .

Considering that the EPR spectra of the Fe^{+} and Fe^{3+} Kramers ions would hardly escape observation, it seems highly probable that the Fe is incorporated into the $CdCl_2$ lattice as Fe^{2+}, whose EPR spectrum is not observed. The incorporation of Fe as substitutional Fe^{2+} ions at Cd^{2+} sites is supported by the same crystal structure ($R\bar{3}m$) of the $FeCl_2$ with $CdCl_2$ and close lattice parameters: $a = 0.3593$ nm and $c = 1.758$ nm for $FeCl_2$ [29].

X-ray irradiation generates mobile holes and electrons. Some holes become trapped at Fe^{2+} to form Fe^{3+} ions. The fact that such centres are produced at low temperatures, where vacancies are expected to be immobile, and with maximum concentration after short irradiation times (10–15 min), suggests that the formation of Fe^{3+} centres consists of simple hole trapping, without involving other lattice defects such as vacancies or interstitials. No such lattice defects seem to be present in the near neighbourhood of the Fe^{3+} centre, as reflected in the trigonal symmetry of its EPR spectrum. Any such neighbouring lattice defect would induce an additional orthorhombic crystal-field component, as well as additional splittings due to non-equivalent positions, which in principle would be easily seen in the $H \perp c$ orientation. The charge compensation of the trapped hole seems to be insured by electrons trapped at lattice sites farther away. No evidence of such electron-trapped centres has been found in either EPR and optical absorption experiments.

The evaluation of the ZFS parameters for the paramagnetic ions with S ground state is a subject of continuing controversy. *Ab initio* calculations for Mn^{2+} in layered structures have failed to account [15, 30] satisfactorily for the absolute values of the most important ZFS parameter b_2^0 . It seems possible, however, to compare the absolute b_2^0 values of the isoelectronic Mn^{2+} and Fe^{3+} ions in hosts with the same crystal lattice . The reference crystal to be considered here is $CaCO_3$ (calcite), which exhibits the same local trigonal symmetry and sixfold coordination at the cation site as $CdCl_2$. The EPR spectra of both substitutional Mn^{2+} and Fe^{3+} have been reported [31, 32]. As presented in table 1 the b_2^0 parameter increases by a factor of 12 from Mn^{2+} to Fe^{3+} in $CaCO_3$ and a factor of 55 in the case of $CdCl_2$. It is indeed expected that for both lattice hosts b_2^0 increases from Mn^{2+} to Fe^{3+}, as a result of the Coulomb attraction of the extrapositive charge, resulting in an inward displacement of the neighbouring ligands toward the Fe^{3+} ion. The additional fivefold increase of the b_2^0 in $CdCl_2$ seems to be due to the specific nature of the chemical bonds in layered compounds. Indeed, the Coulomb attraction exerted by the Fe^{3+} ion on neighbouring Cl^- ligands is much less compensated in $CdCl_2$ by the weak Van der Waals forces from the next layer of Cl^- than in $CaCO_3$, where stronger ionic and covalent bondings between the nearest CO_3^{2-} ligands and the next neighbour ligands are involved.

The above qualitative discussion is further supported by a quantitative analysis of the ZFS parameter b_2^0, based on the SM. Although controversy exists about the validity of this model for $3d^5$ ions, it has proved in many cases useful in determining the local environment of the impurity ion in various lattices [33].

The sc SM provides the following equation for Fe^{3+} at sixfold-coordinated sites with D_{3d} symmetry:

$$b_2^0 = 3\bar{b}_2(R_0)(R_0/R)^{t_2}(3\cos^2\Theta - 1). \tag{3}$$

In this equation $\bar{b}_2(R)$ is an intrinsic parameter that has been found [34, 35] to be -0.61 cm^{-1} at $R_0 = 0.219$ nm for the Fe^{3+}–Cl^- bond in fourfold-coordinated compounds. R is the actual Fe^{3+}–Cl^- distance, Θ is the angle between the Fe^{3+}–Cl^- bond and the c-axis

and $t_2 = 7$.

Considering the parameters $R(Cd^{2+}–Cl^-) = 0.2637$ nm and $\Theta = 56.714°$ corresponding to the pure $CdCl_2$ lattice [3] at RT, one obtains a calculated value of $b_2^0 = 0.048$ cm^{-1}. As previously discussed, we expect the Fe^{3+}–Cl^- distance to be shorter than the Cd^{2+}–Cl^- one, as a result of the Coulomb attraction exercised by the extra positive charge of the Fe^{3+} ion on the chlorine ligands. The smaller ionic radius of the Fe^{3+} ion ($r = 0.064$ nm), compared to Cd^{2+} ($r = 0.097$ nm), will favour this approach, but will also limit it.

Taking the minimum bond length $R(Fe^{3+}–Cl^-) = r(Fe^{3+}) + r(Cl^-) = 0.245$ nm, one obtains $(b_2^0)_{calc} = 0.080$ cm^{-1}. This value is to be compared with the experimental values $b_2^0(13\ K) = 0.0818$ cm^{-1} and $b_2^0(296\ K) = 0.0706$ cm^{-1}, the latter being obtained by a linear extrapolation at 296 K of the experimental b_2^0 values (figure 3). The agreement is remarkably good, considering the approximations involved. The small differences can be easily accounted for by slightly varying the R and/or Θ parameters.

As shown in figure 3 the b_2^0 parameter is strongly temperature dependent. According to the SM this variation can be accounted for by considering the temperature-induced variations in R and/or Θ. Assuming that the interionic distance R is less affected in this temperature range, the changes in b_2^0 will be due a to variation of the angle Θ i.e., to a change in the separation of the Cl^- layers sandwiching the Fe^{3+} ion. Indeed, a simple calculation shows that a reasonable variation of Θ by 0.28° would account for the 0.0112 cm^{-1} variation between 13 K and RT.

Using the SM it is possible to evaluate from the EPR data the thermal expansion coefficient λ_c along the c-axis. A simple geometrical analysis yields the following formula:

$$\lambda_c = \frac{2R(\delta\Theta)\cos\Theta}{d(T_1 - T_2)} \tag{4}$$

where $\delta\Theta$ is the variation of the Θ angle between temperatures T_1 and T_2, and $d = 0.2916$ nm is the separation of the Cl^- layers at RT. A meaningful evaluation has to be made in the temperature range where the expansion coefficient is temperature independent, such as for $T \geqslant T_{Debye}$. This corresponds approximately to the temperatures where b_2^0 is linear [30]. Considering in our calculation the experimental values of $b_2^0(66\ K) = 0.0804$ cm^{-1} and $b_2^0(225\ K) = 0.0736$ cm^{-1}, one finds that $\lambda_c = 1.8 \times 10^{-5}$ K^{-1}. Measurements of thermal expansion of $CdCl_2$, in the temperature range of 300–600 K, resulted [36] in a thermal expansion coefficient $\lambda_z = 8 \times 10^{-5}$ K^{-1} normal to the crystal layers and thermal expansion coefficients along the crystal layers $\lambda_x = \lambda_y < 1 \times 10^{-6}$K^{-1}. The agreement is surprisingly good, considering that a certain elongation of the Fe^{3+}–Cl^- bond length R with temperature is expected and that several other approximations were involved in the calculation.

Concluding this discussion it is worthwhile mentioning that we did not observe EPR transitions due to the hyperfine interaction of the unpaired electrons with the nuclear moment of the ^{57}Fe isotope ($I = \frac{1}{2}$, natural abundance 2.15%). This is not entirely surprising considering that the hyperfine splitting, which is mainly due to core polarization [21], amounts to ≈ 1 mT, which is smaller than the observed linewidths.

5. Conclusions

$CdCl_2$ crystals doped with Fe exhibit after x-ray irradiation paramagnetic centres attributed to Fe^{3+} ions at Cd^{2+} sites. The Fe^{3+} centres result from hole trapping at substitutional Fe^{2+} ions in the $CdCl_2$ lattice. The axial crystal field parallel to the c-axis, to which the Fe^{3+} ion is subjected, is described by a ZFS parameter b_2^0 about 55 times larger than that in the case of Mn^{2+} ions in the same host. It strongly decreases with increase in temperature.

The magnitude of the b_2^0 parameter and its temperature dependence are well described by the SM by considering that the Cl^- ligands next to the Fe^{3+} ion are strongly attracted by its extra positive charge, which results in a reduction of the Fe–Cl separation compared to the Cd–Cl separation in the pure $CdCl_2$. A fair estimation of the thermal expansion coefficient perpendicular to the direction of the lattice layers is obtained with the SM from the variation of b_2^0 in the temperature range of its linear dependence, by taking into consideration an increase in the separation of the Cl layers sandwiching the cations (intralayer expansion).

Acknowledgements

The authors are grateful to Professor J Van Landuyt for permission to use the x-ray diffraction equipment and to Dr A Bouwen and Mrs C D Mateescu for experimental assistance. One of the authors (SVN) is indebted to the Commission of the European Communities for a research scholarship through the Mobility Scheme (Cooperation in Science and Technology with Central and Eastern European Countries). Another author (EG) is a fellow of the Belgian National Fund for Scientific Research (NFWO). This work was supported by the Belgian science supporting agencies IIKW and NFWO.

References

[1] Hulliger F 1976 *Structural Chemistry of Layer-Type Phases* (Dordrecht: Riedel)
[2] Pauling L and Hoard J L 1930 *Z. Kristallogr.* **74** 546
[3] Partin D E and O'Keeffe M 1991 *J. Solid State Chem.* **95** 176
[4] Nistor S V, Ghiordanescu V and Voda M 1976 *Phys. Status Solidi* b **78** K31 and references therein
[5] Hall T P P, Hayes W and Williams F I B 1961 *Proc. Phys. Soc.* **78** 883
[6] Chan I Y, Doetschman D C and Hutchison C A Jr 1965 *J. Chem. Phys.* **42** 1048
[7] Chan K K and Shields L 1970 *J. Phys. C: Solid State Phys.* **3** 292
[8] Morigaki K 1961 *J. Phys. Soc. Japan* **16** 1639
[9] Edgar A 1976 *J. Phys. C: Solid State Phys.* **9** 4303
[10] Partridge M F cited by
Orton J W 1959 *Rep. Prog. Phys.* **23** 204
[11] Iri T and Kuwabara G 1968 *J. Phys. Soc. Japan* **24** 127
[12] Thornley J H M, Magnum B W, Griffiths J H E and Owen J 1961 *Proc. Phys. Soc.* **78** 1263
[13] Matsumoto H 1965 *J. Phys. Soc. Japan* **20** 1579
[14] Kanno K, Naoe S, Mukai S and Nakai Y 1973 *Solid State Commun.* **13** 1325
[15] Edgar A, Siegel E and Urban W 1980 *J. Phys. C: Solid State Phys.* **13** 6649 and references therein
[16] May P S and Güdel H U 1990 *J. Lumin.* **46** 277 and references therein
[17] Voda M, Ghiordanescu V and Pedrini C 1992 *J. Phys.: Condens. Matter* **4** 7145
[18] Bringans R D and Liang W Y 1980 *Physica* B **99** 276
[19] Tubbs M R 1975 *Phys. Status Solidi* b **49** 11; *Phys. Status Solidi* b **67** 11
[20] Goovaerts E, Andriessen J, Nistor S V and Schoemaker D 1981 *Phys. Rev.* B **24** 29
[21] Abragam A and Bleaney B 1970 *Electron Paramagnetic Resonance of Transition Ions* (Oxford: Clarendon)
[22] Nistor S V 1974 *Stud. Cerc. Fiz. (Bucharest)* **9** 1033
[23] Tinkham M 1950 *Proc. R. Soc.* A **236** 549
[24] Nistor S V, Velter-Stefanescu M and Mateescu C D 1985 *Solid State Commun.* **53** 989
[25] Yang B R, Goovaerts E and Schoemaker D 1985 *Phys. Status Solidi* b **127** 657
[26] Nistor S V, Ursu I and Velter-Stefanescu M 1987 *Phys. Rev.* B **35** 4594
[27] Hall T P P, Hayes W, Stevenson R W H and Wilkens J 1963 *J. Chem. Phys.* **38** 1977
[28] Nistor S V 1969 *PhD Thesis* University of Cluj
[29] Ferrari A, Braibanti A and Bigliardi G 1963 *Acta Crystallogr.* **16** 846
[30] Glinchuk V E, Goncharuk V E, Lyfar D L and Ryabchenko S M 1976 *Sov. Phys.–Solid State* **18** 7
[31] Hodges J A, Marshall S A, McMillan J A and Serway R A 1968 *J. Chem. Phys.* **49** 2857
[32] Marshall S A and Reinberg A R 1963 *Phys. Rev.* **132** 134
[33] Newman D J and Ng B 1989 *Rep. Prog. Phys.* **132** 134

[34] Büscher R, Lehman G, Henkel G and Krebs B 1984 *Z. Naturf.* a **39** 1204
[35] Büscher R and Lehman G 1987 *Z. Naturf.* a **42** 67
[36] Sharma R R 1971 *Phys. Rev.* B **3** 76